Video Article

Preparation and Photoacoustic Analysis of Cellular Vehicles Containing Gold Nanorods

Lucia Cavigli[1], Francesca Tatini[1], Claudia Borri[2], Fulvio Ratto[1], Sonia Centi[1], Alberto Cini[3], Beatrice Lelli[4], Paolo Matteini[1], Roberto Pini[1]

[1]Institute of Applied Physics, Italian National Research Council

[2]Department of Experimental and Clinical Biomedical Sciences, University of Florence, Firenze

[3]Department of Physics and Astronomy, University of Florence, Sesto Fiorentino

[4]Department of Pharmacy and Biotechnology, University of Bologna

Correspondence to: Fulvio Ratto at f.ratto@ifac.cnr.it

URL: https://www.jove.com/video/53328
DOI: doi:10.3791/53328

Keywords: Bioengineering, Issue 111, Plasmonic particles, Gold nanorods, Chitosan, Cellular vehicles, Macrophages, Photoacoustic microscopy, Photostability

Date Published: 5/2/2016

Citation: Cavigli, L., Tatini, F., Borri, C., Ratto, F., Centi, S., Cini, A., Lelli, B., Matteini, P., Pini, R. Preparation and Photoacoustic Analysis of Cellular Vehicles Containing Gold Nanorods. *J. Vis. Exp.* (111), e53328, doi:10.3791/53328 (2016).

Abstract

Gold nanorods are attractive for a range of biomedical applications, such as the photothermal ablation and the photoacoustic imaging of cancer, thanks to their intense optical absorbance in the near-infrared window, low cytotoxicity and potential to home into tumors. However, their delivery to tumors still remains an issue. An innovative approach consists of the exploitation of the tropism of tumor-associated macrophages that may be loaded with gold nanorods *in vitro*. Here, we describe the preparation and the photoacoustic inspection of cellular vehicles containing gold nanorods. PEGylated gold nanorods are modified with quaternary ammonium compounds, in order to achieve a cationic profile. On contact with murine macrophages in ordinary Petri dishes, these particles are found to undergo massive uptake into endocytic vesicles. Then these cells are embedded in biopolymeric hydrogels, which are used to verify that the stability of photoacoustic conversion of the particles is retained in their inclusion into cellular vehicles. We are confident that these results may provide new inspiration for the development of novel strategies to deliver plasmonic particles to tumors.

Video Link

The video component of this article can be found at https://www.jove.com/video/53328/

Introduction

Over the past decade, various plasmonic particles such as gold nanorods, nanoshells and nanocages, have received considerable attention for applications in biomedical optics[1,2,3,4]. At variance with standard gold nanospheres, these newer particles resonate in the near infrared (NIR) window that provides for deepest optical penetration through the body and highest optical contrast over endogenous components[1]. This feature has aroused interest for innovative applications, such as the photoacoustic (PA) imaging and the photothermal ablation of cancer. However, several issues restrain the clinical penetration of these particles. For instance, their optical activation tends to induce their overheating and to modify their functional shapes towards more spherical profiles, which drives a photoinstability[5,6,7,8,9]. Another issue that dominates the scientific debate is their systemic delivery into tumors. In particular, gold nanorods combine sizes that are ideal to pervade tumors that display enhanced permeability and retention and ease of conjugation with specific probes of malignant markers. Therefore, their preparation for a direct injection into the bloodstream is perceived as a feasible scheme[10,11,12,13]. However, this route remains problematic, with most of the particles becoming captured by the mononuclear phagocyte system[10,11,12]. In addition, another concern is the optical and biochemical stability of the particles after circulation through the body[14]. When particles lose their colloidal stability and aggregate, their plasmonic features and heat transfer dynamics may suffer from plasmonic coupling[15,16,17] and cross-overheating[18].

More recently, the notion to exploit the tropism of tumor-associated macrophages has emerged as a smart alternative[19,20,21]. These cells hold an innate ability to detect and pervade tumors with high specificity. Therefore, one perspective may be to isolate these cells from a patient, load them with gold nanorods *in vitro* and then inject them back into the patient, with the intent to use them as cellular vehicles in charge of the delivery. Another advantage would be to gain more control over the optical and biochemical stability of the particles, because their biological interface would be constructed *in vitro*. Still, the performances of these cellular vehicles as optical contrast agents need a critical analysis.

In this work, we describe the preparation and critical issues of cellular vehicles containing gold nanorods for the PA imaging of cancer. PEGylated gold nanorods are modified with quaternary ammonium compounds[22], in order to achieve a cationic profile that is expected to promote their interactions with plasmatic membranes[23,24]. These particles undergo efficient and unspecific uptake from most cellular kinds, hopefully without interfering much with their biological functions. Murine macrophages are loaded with up to as many as 200,000 cationic gold nanorods per cell, which become confined within tight endocytic vesicles. This configuration should arise concern, because of the threat of plasmonic coupling and cross-overheating inside these vesicles. Therefore, the macrophages are embedded in biopolymeric hydrogels that mimic biological tissues,

in order to verify that most of the stability of PA conversion of the particles is retained in the transfer from the growth medium to the endocytic vesicles. Effective measurement criteria are worked out in order to measure the stability of PA conversion under conditions of immediate interest for PA imaging. A reshaping threshold is set at the very onset of optical instability after a train of 50 laser pulses with the typical repetition rate of 10 Hz.

We are confident that these results may provide momentum for the development of novel strategies to deliver plasmonic particles to tumors.

Protocol

Note: All concentrations of gold nanorods are expressed in terms of nominal Au molarities. For comparison with other works, note that 1 M Au roughly corresponds to 20 µM gold nanorods, in our case.

1. Preparation of Cationic Gold Nanorods

Note: The method begins with the synthesis of cetrimonium bromide (CTAB)-capped gold nanorods by the autocatalytic reduction of $HAuCl_4$ with ascorbic acid, according to the protocol introduced by Nikoobakht *et al.*[25] and adapted according to Ratto *et al.*[26]. Then these gold nanorods are modified in order to gain more biocompatibility and affinity for plasmatic membranes, by the combination of polyethylene glycol strands[10,11,27,28] and quaternary ammonium compounds[22].

1. Purify 24 ml CTAB-capped gold nanorods at a concentration of 450 µM Au by two cycles of centrifugation (12,000 x g, 30 min) and decantation. Make sure that the ratio of dead volume to initial volume is around 1/200 or lower for all centrifugation steps in this protocol. Use 500 µM aqueous CTAB as a washing solution and finally transfer the particles into 6 ml 100 mM acetate buffer at pH 5 containing 500 µM CTAB and 0.005% (v/v) polysorbate 20.
2. Add 30 µl 10 mM aqueous alpha-methoxy-omega-mercapto-poly(ethylene glycol) (MW ~ 5,000) and leave to react for 30 min at 37 °C.
3. Add 30 µl 100 mM (11-Mercaptoundecyl)-*N,N,N*-trimethylammonium bromide in dimethyl sulfoxide and leave at rest for 24 hr at 37 °C.
4. Next, add 18 ml 0.005% (v/v) polysorbate 20 in water and purify these particles by four cycles of centrifugation (12,000 x g, 30 min) and decantation. Use 0.005% (v/v) polysorbate 20 in water as washing solution and finally transfer the particles into 2.4 ml sterile PBS at pH 7.4. The final nominal concentration of gold is 4.5 mM.

2. Loading of Murine Macrophages with Gold Nanorods

1. Use the monocyte/macrophagic cell line J774a.1 and DMEM supplemented with 10% fetal bovine serum, 1 mM glutamine, 100 units/ml penicillin and 100 µg/ml streptomycin as culture medium. Plate 5 x 10^5 cells in four Petri dishes of 60 mm diameter and allow them to grow for 24 hr, so as to be subconfluent at the time of detachment (see step 2.2).
    1. Throughout the protocol, maintain the cells under standard culture conditions (37 °C, 5% CO_2, 95% air and 100% relative humidity). Use a laminar flow cabinet and appropriate personal protective equipment to manipulate the cells.

2. After 24 hr, load the cells with cationic gold nanorods and prepare them to be embedded into chitosan films:
    1. In order to allow the particles to be taken up by the cells, add an aliquot of 4.5 mM Au cationic gold nanorods in PBS into each Petri dish, so as to achieve a final concentration of 100 µM Au. Leave the Petri dishes in incubation for 24 hr.
    2. Next, observe the cells under an optical microscope to confirm their good conditions and the upload. Cells should exhibit their normal morphology and a number of dark intracellular vesicles. Detach the cells by a scraper, merge those from two Petri dishes, in order to achieve a suitable amount of cells for the following steps (at least 2 x 10^6 cells), and centrifuge them (120 x g, 6 min) to eliminate any excess of cationic gold nanorods. The cellular pellet should look almost black.
    3. Suspend the pellet in 2 ml PBS and count the cells by the use of a Bürker chamber. Centrifuge a suspension containing 2 x 10^6 cells (120 x g, 6 min) and fix their pellet in 2 ml 3.6% (w/v) formaldehyde in PBS for ten minutes at room temperature. Finally, wash this pellet three times by centrifugation (120 x g, 6 min) in order to remove the fixative. Use PBS as washing solution.

3. Embedment of Macrophages into Chitosan Films

Note: The peculiar properties of chitosan[26,27,28,29] are exploited to produce biomimetic phantoms containing macrophages stained with cationic gold nanorods. With respect to other hydrogels such as agarose, chitosan enables films that are much stronger and thinner, which is critical for PA microscopy[6]. The fabrication of these phantoms is carried out according to previous protocols[29,30,31] with some modifications as prescribed in the followings[30].

1. Prepare an acidified (pH 4.5, obtained by the addition of acetic acid) and viscous 3% (w/v) low molecular weight chitosan (average MW 120 kDa) solution, thoroughly mix it and let it homogenize for 24 hr at 40 °C.
2. Next, mix murine macrophages containing cationic gold nanorods (2 x 10^6 cells) with 500 µl of chitosan solution.
3. In order to obtain ~50 µm thick phantoms, pour 250 mg of the mixture into 1.91 cm^2 polystyrene molds and leave them under a nitrogen stream for 24 hr. Thereafter, treat these samples with 500 µl 1 M NaOH, in order to induce cross-linking, and rinse them with 10 ml of ultrapure water.

4. Test of the Stability of Photoacoustic Conversion

Note: The stability of PA conversion is investigated by means of PA experiments with the home-made setup that is described in ref 6.

1. Suspend a chitosan film containing the macrophages in DI water, for instance by the use of a plastic holder immersed in a Petri dish, so as to keep a distance of ~5 mm from the bottom of the plate. Put this plate onto a micrometric XY stage in order to control the sample position.
2. Focus a laser beam with ~5 nsec pulse duration in resonance with the longitudinal plasmonic band of the gold nanorods (*e.g.*, from an optical parametric oscillator pumped by the third harmonic of a Q-switched Nd:YAG laser with wavelength range of 400 - 2,500 nm and pulse duration of 5 nsec) perpendicular to the film surface with a ~300 µm spot diameter.
    1. Place an attenuator in front of the laser exit to tune the laser fluence and use a beam splitter to focus part of the laser beam to an energy meter (*e.g.*, a pyroelectric detector) and monitor fluence fluctuations. Maintain the optical fluence below ~1 mJ/cm^2 per pulse during the alignment. Use appropriate laser safety eyewear whenever the laser is on.
3. Dip an ultrasound transducer (frequency range of 1 - 20 MHz) into the Petri dish ~2 mm off of the film surface and adjust its position by using micrometric translations and rotational stages to maximize the PA signal emitted from the film.
4. Determine a probe fluence F_{LO} that does not damage the sample[6]:
    1. Irradiate a random point of the sample at a fluence around 1 mJ/cm^2 per pulse for at least 500 pulses. For each pulse, acquire the corresponding PA signal from the ultrasound transducer and laser fluence from the energy meter with an oscilloscope. Name the average fluence as F_{LO}^{trial}.
    2. Calculate the intensity of the PA signal as its peak-to-peak amplitude as a function of pulse number. In order to counterweight the laser intensity fluctuations, normalize the amplitude of each PA signal to the ratio of its own fluence to F_{LO}^{trial}. Analyze the trend of the normalized PA intensity as a function of pulse number and verify its stability over time.
    3. In the case of instability, repeat steps 4.4.1 to 4.4.3 with a lower value of F_{LO}^{trial}. In the case of stability, repeat them with a value of F_{LO}^{trial} higher by ~10%, until a loss of stability arises. Set the probe fluence F_{LO} as the second highest value of F_{LO}^{trial} that ensures stability.
5. Measure a reshaping threshold fluence:
    1. Choose another random point of the sample and probe an average PA intensity (I_{LO}^{a}) over 500 pulses at F_{LO}.
    2. Set a nominal fluence greater than F_{LO} and deliver 50 pulses. Name their average fluence as F_{exc}.
    3. Probe an average PA intensity (I_{LO}^{b}) over 500 pulses at F_{LO} once again. Calculate the ratio $R = I_{LO}^{b} / I_{LO}^{a}$. A value of R below unity gives evidence of an irreversible change of the optical properties of the sample.
    4. Use the micrometric XY stage to move the film and change the point of the sample at random. Repeat steps 4.5.1 to 4.5.4 with different values of F_{exc}, so as to take a few values of R below, around and above unity. 15 points are reasonable.
    5. Plot R as a function of F_{exc} and identify the reshaping threshold fluence F_{th} as that value when R begins to differ from one beyond statistical uncertainty.[6]

Representative Results

Here, the feasibility of cellular vehicles containing gold nanorods for the PA imaging of cancer is shown together with typical outcomes of the protocol.

The TEM images in **Figure 1** show the usual appearance of the particles after step 1 and their cellular vehicles after step 2. The preparation of the particles and of the cells for TEM imaging is described elsewhere[17]. Cationic gold nanorods undergo a massive accumulation in macrophages, which maintain their normal morphology. Particles are found to be confined within tight endocytic vesicles.

Figure 2a displays an optical transmission image of macrophages containing cationic gold nanorods and dispersed in a chitosan phantom after step 3. As proven by this micrograph, the inclusion in the chitosan hydrogel does not affect the cellular morphology. Cells are well dispersed throughout the sample. Controls of chitosan films containing gold nanorods without cells are homogeneous. **Figure 2b** shows that the typical plasmonic band of gold nanorods is retained when the particles are taken up by the macrophages, consistent with our previous work[14,32]. Therefore, effects such as plasmonic coupling on segregation in endocytic vesicles and a differential uptake of particles with different size and shape that coexist in a polydisperse colloid[28,33] do not play a substantial role in these protocols. **Figure 2b** also proves the feasibility of chitosan as an optical phantom.

Figure 3 shows the trend of R as a function of F_{exc} measured according to step 4 and gives an idea of the data and the analysis that are required for the determination of F_{th} as per step 4.5.5. F_{th} was found to be (11 ± 1) mJ/cm^2 in this example. PA measurements on this sample gave signals with signal to noise ratio (SNR) greater than 20 when averaged over 500 pulses at few mJ/cm^2, which provides high accuracy for the investigation of the stability of PA conversion from the cellular vehicles.

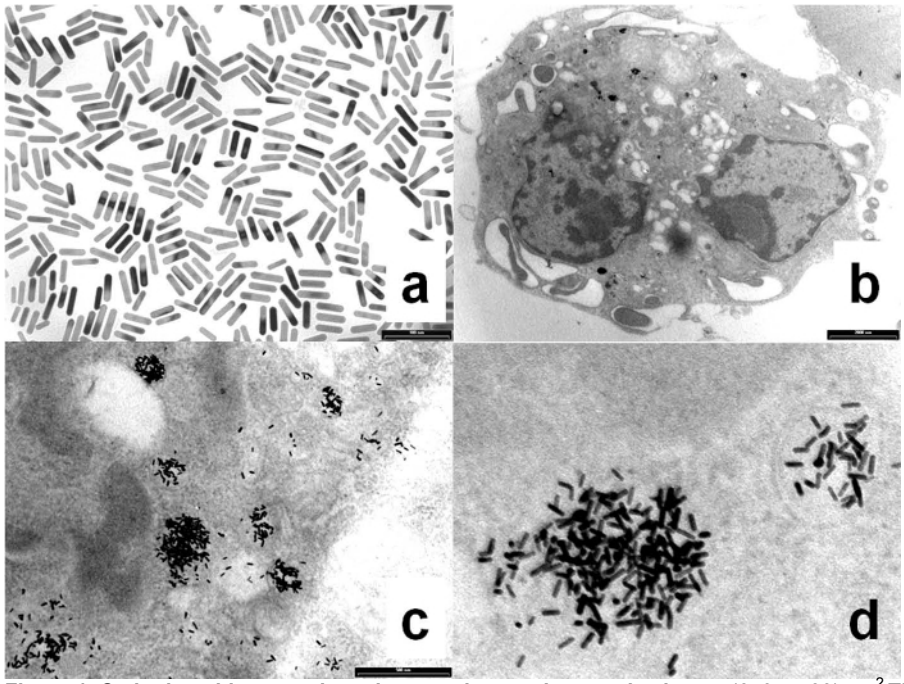

Figure 1. Cationic gold nanorods and macrophages characterization. a: (650 × 500) nm^2 TEM image of as-synthesized gold nanorods; **b**, **c** and **d**: respectively (13 × 8.6) μm^2, (2.3 × 1.7) μm^2 and (870 × 650) nm^2 TEM images of macrophages treated with cationic gold nanorods. The appearance of the particles in panel d is affected by their inclination in the cell. Please click here to view a larger version of this figure.

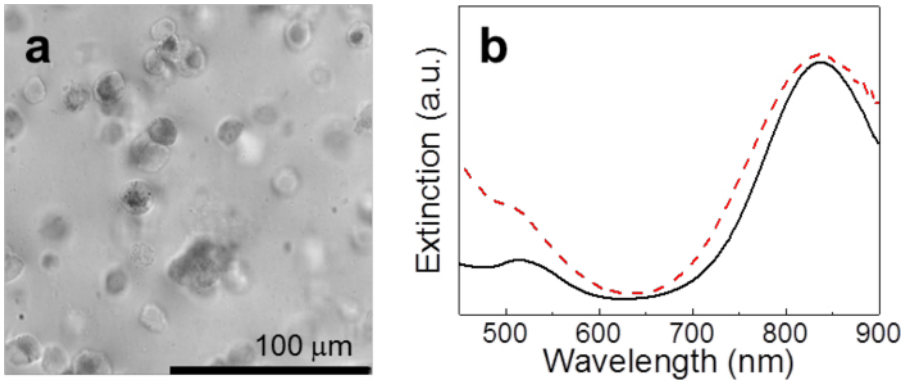

Figure 2. Chitosan film characterization. a: Optical transmission image of macrophages containing cationic gold nanorods and dispersed in a chitosan phantom. **b**: Optical extinction spectra of chitosan phantoms containing gold nanorods without cells (solid black line, control sample) and macrophages containing gold nanorods (broken red line). Please click here to view a larger version of this figure.

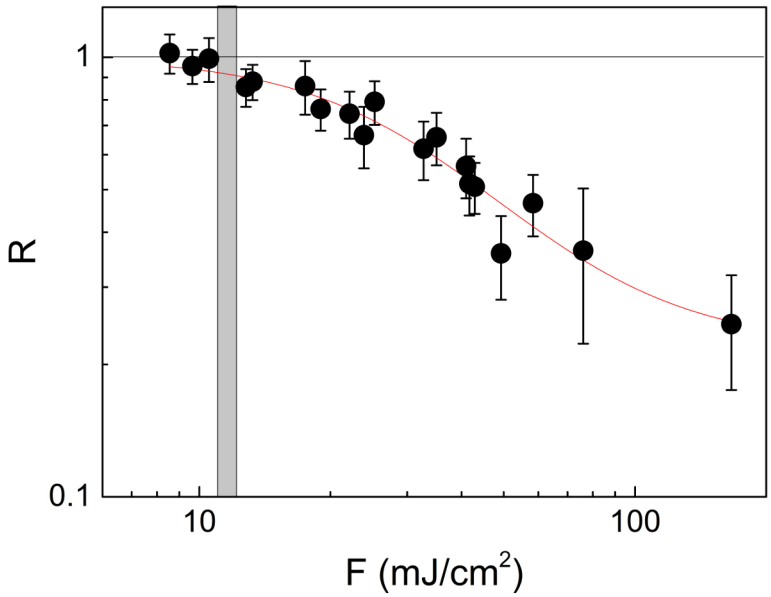

Figure 3. Cellular vehicles photostability. Ratio R of the intensities of I_{LO} taken after and before irradiation at each F_{exc} versus F_{exc}. The error bars originate from the signal fluctuations at F_{LO}. The reshaping threshold is extracted from these data as R falls below unity. The red solid line serves as a guide to the eye. Please click here to view a larger version of this figure.

Discussion

The notion to target tumor-associated macrophages is emerging as a powerful concept to combat cancer[34,35,36]. Here, instead of their destruction, these cells are recruited as cellular vehicles to bring gold nanorods into a tumor, by the exploitation of their tropism. This perspective requires a thoughtful design of the particles, their integration into the cells and their characterization. We have found that the photostability of murine macrophages loaded with cationic gold nanorods does not suffer from the confinement of particles within endocytic vesicles, which implies that their plasmonic coupling and cross-overheating are not critical. We hypothesize that the PEG strands and the incidence of shapes that are off-resonance, such as gold nanospheres, prevent the particles to get into too tight contact, which is about their diameters[17] (around 10 nm) and one thermal diffusion length (around 30 nm in 5 nsec) for plasmonic coupling and cross-overheating, respectively.

The protocol is innovative with respect to existing methods in the design of the particles and of the investigation of their photostability. The design of gold nanorods according to step 1 combines the observation by Vigderman *et al.*[22] that quaternary ammonium compounds are capable to drive a massive uptake of gold nanorods into endocytic vesicles and the notion that cell penetrating agents with a cationic profile[24,37] may be embedded within a PEG shell[38] and remain functional, while gaining colloidal stability and biocompatibility[28]. Indeed step 1 resembles the method by Yuan *et al.*[38], with the replacement of cell penetrating peptides with smaller and cheaper quaternary ammonium compounds. With these modifications, cationic gold nanorods are multifunctional and sustainable. Since these particles are intended as contrast agents for PA imaging, a PA probe is ideal to test their functional features. The measurement of the stability of PA conversion by the definition of a reshaping threshold in step 4 is quantitative and reproducible, which are unique features in the frame of the scientific literature. Besides, we note that this method does not require a calibration of the PA equipment.

Critical steps within the protocol include the fabrication of the chitosan films to inspect the cellular vehicles in terms of their efficiency as contrast agents for PA imaging. Chitosan is a linear chain biopolymer comprising glucosamine and *N*-acetyl glucosamine residues joined together by 1,4-glycosidic bonds. Some physiochemical features of chitosan, such as its pore size, porosity and mechanical properties, as well as its versatility and handiness, make it an ideal option for the fabrication of hydrogels in the form of thin films or porous membranes[29,39,40]. Moreover, the polysaccharide backbone of chitosan is structurally similar to glycosaminoglycans, the major component of the extra-cellular matrix of connective tissues, which has promoted its use for engineering biomimetic and cell-supporting scaffolds[41]. Overall, chitosan hydrogels exhibit thermal and elastic moduli that are representative of connective tissue[29,41,42], which is ideal for PA tests. Care should be taken to achieve films with the proper thickness (50 µm), low optical turbidity and good homogeneity. Note that the doses given in step 3 have been optimized. The viscous suspension of murine macrophages in chitosan should be mixed with diligence according to step 3.2. With these instructions, these films have already been used to compare the stability of PA conversion of gold nanorods of different size[6].

Possible modifications of the protocol include the preparation of the cationic gold nanorods and cellular vehicles in steps 1 and 2. The method in step 1 may be subject to incremental improvements, *e.g.*, by the substitution of the cell penetrating agent or the length of the PEG strands *etc.*, in order to minimize any interference with the physiology of the tumor-associated macrophages. The use of ligands that are specific for macrophages may be an option[43]. Other parameters that affect the uptake of the particles include their size and shape[33] and their inorganic coating. For instance, a shell of silica may give a combination of high internalization[44], optical stability against aggregation[17] and PA stability[7], at the expense of more sophistication and more foreign material. We conjecture that the endosomal pathway of internalization may be a common effect[33,43,44,45]. A critical examination of the cells from step 2 is underway and the best arrangement of optical contrast, viability and chemotactic activity *in vitro* and *in vivo* may still require to adjust the dosage of the plasmonic particles in terms of concentration and duration of the incubation. Although the morphology of the cells and the preliminary evidence in our hands suggest a low cytotoxicity, the investigation of these parameters is beyond the scope of this work. Another perspective would be to reproduce step 2 with other cells of the immune system[46]

and primary cells, which may be chosen on a case-by-case basis. Indeed, we speculate that the notion to modulate the uptake of the particles with their electrokinetic potential is most versatile.

Limitations of the protocol include the need to use fixed cells rather than live cells, because the prescriptions in step 3 are incompatible with the preservation of cellular viability. Other restrictions relate to the need of a sufficient SNR in the determination of a probe fluence in step 4.4, which translates into a sufficient combination of optical absorbance and photostability of the film.

In conclusion, we have described an innovative protocol to prepare and to perform a functional characterization of cellular vehicles that are feasible as contrast agents for photoacoustic imaging. We have found that the introduction of gold nanorods into murine macrophages does not negatively affect their photostability. The focus of our current work is on the physiology of these cells, with a special attention for their viability and chemotactic activity. In the future, this method shall be tested to investigate the preparation of different cellular vehicles containing different solutions of optical contrast agents. The PA probe may also serve to test the targetability of optical contrast agents to malignant cells *in vitro*, without the use of cellular vehicles.

Disclosures

The authors declare that they have no competing financial interests.

Acknowledgements

This work was partially supported by Regione Toscana and European Community within the frame of the ERANET+ Projects LUS BUBBLE and BI-TRE.

References

1. Ratto, F., Matteini, P., Centi, S., Rossi, F., & Pini, R. Gold nanorods as new nanochromophores for photothermal therapies. *J. Biophotonics.* **4**(1-2), 64-73 (2011).
2. Dreaden, E. C., Alkilany, A. M., Huang, X., Murphy, C. J., & El-Sayed, M. A. The golden age: gold nanoparticles for biomedicine. *Chem. Soc. Rev.* **41**, 2740-2779 (2012).
3. Hahn, M. A., Singh, A. K., Sharma, P., Brown, S. C., & Moudgil, B. M. Nanoparticles as Contrast Agents for in-Vivo Bioimaging: Current Status and Future Perspectives. *Anal. Bioanal. Chem.* **399**(1), 3-27 (2011).
4. Dreaden, E. C., Austin, L. A., Mackey, M. A., & El-Sayed, M. A. Size matters: gold nanoparticles in targeted cancer drug delivery. *Ther. Deliv.* **3**(4), 457-478 (2012).
5. Manohar, S., Ungureanu, C., & Van Leeuwen, T. G. Gold nanorods as molecular contrast agents in photoacoustic imaging: The promises and the caveats. *Contrast Media Mol. Imaging.* **6 (5)**, 389-400 (2011).
6. Cavigli, L., *et al.* Size Affects the Stability of the Photoacoustic Conversion of Gold Nanorods. *J. Phys. Chem. C* **118**(29), 16140-16146 (2014).
7. Chen, L.-C., *et al.* Enhanced photoacoustic stability of gold nanorods by silica matrix confinement. *J. Biomed. Opt.* **15**(1), 016010 (2010).
8. Ratto, F., *et al.* CW laser-induced photothermal conversion and shape transformation of gold nanodogbones in hydrated chitosan films. *J. Nanopart. Res.* **13**, 4337-4348 (2011).
9. Mercatelli, R., *et al.* Quantitative readout of optically encoded gold nanorods using an ordinary dark-field microscope. *Nanoscale* **5**(20) 9645-50 (2013).
10. Von Maltzahn, G., *et al.* Computationally guided photothermal tumor therapy using long-circulating gold nanorod antennas. *Cancer Res.* **69**(9), 3892-3900 (2009).
11. Jokerst, J. V., Cole, A. J., Van De Sompel, D., & Gambhir, S. S. Gold nanorods for ovarian cancer detection with photoacoustic imaging and resection guidance via Raman imaging in living mice. *ACS Nano.* **6**(11), 10366-10377 (2012).
12. Huang, X., *et al.* A reexamination of active and passive tumor targeting by using rod-shaped gold nanocrystals and covalently conjugated peptide ligands. *ACS Nano* **4**(10), 5887-5896 (2010).
13. Alkilany, A. M., Thompson, L. B., Boulos, S. P., Sisco, P. N., & Murphy, C. J. Gold nanorods: Their potential for photothermal therapeutics and drug delivery, tempered by the complexity of their biological interactions. *Adv. Drug Deliv. Rev.* **64**, 190-199 (2012).
14. Centi, S., *et al.* In vitro assessment of antibody-conjugated gold nanorods for systemic injections. *J. Nanobiotechnology* **12**, 55 (2014).
15. Jain, P. K., Eustis, S., & El-Sayed, M. A. Plasmon coupling in nanorod assemblies: Optical absorption, discrete dipole approximation simulation, and exciton-coupling model. *J. Phys. Chem. B.* **110**(37) 18243-18253 (2006).
16. Funston, A. M., Novo, C., Davis, T. J., & Mulvaney, P. Plasmon coupling of gold nanorods at short distances and in different geometries. *Nano Lett.* **9**(4) 1651-1658 (2009).
17. Mazzoni, M., Ratto, F., Fortunato, C., Centi, S., Tatini, F., & Pini, R. Partial Decoupling in Aggregates of Silanized Gold Nanorods. *J. Phys. Chem. C.* **118**(34) 20018-20025 (2014).
18. Lapotko, D. O., Lukianova, E., & Oraevsky, A. A. Selective laser nano-thermolysis of human leukemia cells with microbubbles generated around clusters of gold nanoparticles. *Lasers Surg. Med.* **38**(6) 631-642 (2006).
19. Choi, M. R., *et al.* A cellular trojan horse for delivery of therapeutic nanoparticles into tumors. *Nano Letters* **7**(12) 3759-3765 (2007).
20. Dreaden, E. C., Mwakwari, S. C., Austin, L. a., Kieffer, M. J., Oyelere, A. K., & El-Sayed, M. a. Small molecule-gold nanorod conjugates selectively target and induce macrophage cytotoxicity towards breast cancer cells. *Small.* **8**(18) 2819-2822 (2012).
21. Yang, T. D., *et al.* Real-time phase-contrast imaging of photothermal treatment of head and neck squamous cell carcinoma: an in vitro study of macrophages as a vector for the delivery of gold nanoshells. *J. Biomed. Opt.* **17**(12) 128003 (2012).
22. Vigderman, L., Manna, P., & Zubarev, E. R. Quantitative Replacement of Cetyl Trimethylammonium Bromide by Cationic Thiol Ligands on the Surface of Gold Nanorods and Their Extremely Large Uptake by Cancer Cells. *Angew. Chem. Int. Ed. (English).* **51**(3) 636-641 (2012).
23. Richard, J. P., *et al.* Cell-penetrating peptides: A reevaluation of the mechanism of cellular uptake. *J. Biol. Chem.* **278**(1) 585-590 (2003).

24. Delehanty, J. B., Boeneman, K., Bradburne, C. E., Robertson, K., Bongard, J. E., & Medintz, I. L. Peptides for specific intracellular delivery and targeting of nanoparticles: implications for developing nanoparticle-mediated drug delivery. *Ther. Deliv.* **1**, 411-433 (2010).
25. Nikoobakht, B., & El-Sayed, M. A. Preparation and growth mechanism of gold nanorods (NRs) using seed-mediated growth method. *Chem. Mater.* **15**(10) 1957-1962 (2003).
26. Ratto, F., Matteini, P., Rossi, F., & Pini, R. Size and shape control in the overgrowth of gold nanorods. *J. Nanopart. Res.* **12**(6) 2029-2036 (2009).
27. Niidome, T., *et al.* PEG-modified gold nanorods with a stealth character for in vivo applications. *J. Control. Release* **114**(3) 343-347 (2006).
28. Tatini, F., *et al.* Size dependent biological profiles of PEGylated gold nanorods. *J. Mater. Chem. B* **2**, 6072-6080 (2014).
29. Matteini, P., Ratto, F., Rossi, F., Centi, S., Dei, L., & Pini, R. Chitosan films doped with gold nanorods as laser-activatable hybrid bioadhesives. *Adv. Mater.* **22**(38) 4313-6 (2010).
30. Matteini, P., Ratto, F., Rossi, F., de Angelis, M., Cavigli, L., & Pini, R. Hybrid nanocomposite films for laser-activated tissue bonding. *J. Biophotonics.* **5**(11-12) 868-77 (2012).
31. Matteini, P., Tatini, F., Cavigli, L., Ottaviano, S., Ghini, G., & Pini, R. Graphene as a photothermal switch for controlled drug release. *Nanoscale.* **6**, 7947-7953 (2014).
32. Ratto, F., Witort, E., *et al.* Plasmonic Particles that Hit Hypoxic Cells. *Adv. Funct. Mater.* **25**(2) 316-323 (2015).
33. Chithrani, D. B. Intracellular uptake, transport, and processing of gold nanostructures. *Molec. Membrane Biol.* **27**(7) 299-311 (2010).
34. Mitchem, J. B., *et al.* Targeting tumor-infiltrating macrophages decreases tumor-initiating cells, relieves immunosuppression, and improves chemotherapeutic responses. *Cancer Res.* **73**(3) 1128-1141 (2013).
35. Mantovani, A., & Allavena, P. The interaction of anticancer therapies with tumor-associated macrophages. *J. Exp. Med.* **212**(4) 435-445 (2015).
36. Panni, R. Z., Linehan, D. C., & DeNardo, D. G. Targeting tumor-infiltrating macrophages to combat cancer. *Immunotherapy.* **5**(10) 1075-87 (2013).
37. Oh, E., *et al.* Cellular uptake and fate of PEGylated gold nanoparticles is dependent on both cell-penetration peptides and particle size. *ACS Nano* **5**(8) 6434-6448 (2011).
38. Yuan, H., Fales, A. M., & Vo-Dinh, T. TAT peptide-functionalized gold nanostars: Enhanced intracellular delivery and efficient NIR photothermal therapy using ultralow irradiance. *J. Am. Chem. Soc.* **134**(28) 11358-11361 (2012).
39. Ladet, S., David, L., & Domard, A. Multi-membrane hydrogels. *Nature.* **452**, 76-79 (2008).
40. Matteini, P., *et al.* Photothermally activated hybrid films for quantitative confined release of chemical species. *Angew. Chem. Int. Ed. (English)* **52**, 5956-5960 (2013).
41. Khor, E., & Lim, L. Y. Implantable applications of chitin and chitosan. *Biomaterials.* **24**(13) 2339-2349 (2003).
42. Kennedy, L. C., *et al.* T cells enhance gold nanoparticle delivery to tumors in vivo. *Nanoscale Res. Lett.* **6**(1) 283 (2011).
43. Pissuwan, D., Valenzuela, S. M., Killingsworth, M. C., Xu, X., & Cortie, M. B. Targeted destruction of murine macrophage cells with bioconjugated gold nanorods. *J. Nanopart. Res.* **9**(6) 1109-1124 (2007).
44. Jokerst, J. V., Thangaraj, M., Kempen, P. J., Sinclair, R., & Gambhir, S. S. Photoacoustic imaging of mesenchymal stem cells in living mice via silica-coated gold nanorods. *ACS Nano.* **6**(7) 5920-5930 (2012).
45. Ding, H., *et al.* Gold nanorods coated with multilayer polyelectrolyte as contrast agents for multimodal imaging. *J. Phys. Chem. C* **111**(34) 12552-12557 (2007).
46. Esposito, G., *et al.* In vivo laser assisted microvascular repair and end-to-end anastomosis by means of indocyanine green-infused chitosan patches: A pilot study. *Lasers Surg. Med.* **45**(5), 318-325 (2013).

